Hindawi
International Journal of Photoenergy
Volume 2022, Article ID 4713869, 9 pages
https://doi.org/10.1155/2022/4713869

Research Article

Demonstrating and Investigating the Mechanical Strength of Solar Cells

V. Ravi Raj,[1] R. Krishna Priya,[2] K. V. Bindu,[3] N. Prabhu,[4] S. Madhavarao,[5] G. Ramkumar,[6] A. H. Seikh,[7] M. H. Siddique,[8] and Endalkachew Mergia Anbese[9]

[1]*Department of Mechanical Engineering, Sri Sairam Engineering College, Chennai, 600044 Tamil Nadu, India*
[2]*Deanship of PG and Research, National University of Science and Technology, Muscat, Oman*
[3]*Department of Electrical & Electronics Engineering, RMK College of Engineering and Technology, Chennai, India*
[4]*Department of Mechanical Engineering, PSN Engineering College, Melathediyoor, Tirunelveli, 627152 Tamil Nadu, India*
[5]*Department of Mechanical Engineering, Sagi Ramakrishnam Raju Engineering College, Bhimavaram, 534204 Andhra Pradesh, India*
[6]*Department of Electronics and Communication Engineering, Saveetha School of Engineering, SIMATS, Chennai, Tamil Nadu, India*
[7]*Mechanical Engineering Department, College of Engineering, King Saud University, Saudi Arabia*
[8]*Department of Industrial Engineering, Yonsei University, Seoul, Republic of Korea*
[9]*Department of Civil Engineering, Ambo University, Ambo, Ethiopia*

Correspondence should be addressed to Endalkachew Mergia Anbese; endalkachew.mergia@ambou.edu.et

Received 14 June 2022; Revised 6 August 2022; Accepted 10 August 2022; Published 19 September 2022

Academic Editor: B.R. Ramesh Bapu

This study reports on the silicon photovoltaic cells with such an alumina metallization. The photovoltaic cell's silicon component was subjected to an effective stress studied using a simulation model built with this information. In order to evaluate the efficiency of photovoltaic cells on both sides, as well as in two distinct orientations, a four-point bending experiment analysis was carried out using the model. The side and direction of loading have a significant impact on both strength and fracture. There is tensile stress going perpendicularly along the busbars; the back side of the test specimen had the lowest measured strength.

1. Introduction

In the collection and management of solar power systems, mechanical integrity is critical [1]. There is a lot of interest in fractures in modules because mechanical or thermal stress can drastically affect the module's electrical efficiency and reliability [2]. According to the loads, the tipping point or ultimate strength for the solar cell fracture must be evaluated, despite the fact that there are several factors that contribute to cell breakdown, but they are only one of them [3]. This strength is further characterized by the specific fault structure that emerges during the production methodology for cells, which begins the silicon wafering process [4]. However, defects in silicon wafers and the tensile strength solar cells have been extensively studied. The interfacial fracture behaviour of photovoltaic cells determines how quickly photoelectric array's cells break down [5, 6], with little attention to solar panel quality consideration. Si, Al, and Ag [7] are all components that can be found in current silicon solar cells; analyzing each layer's contribution to cell strength is necessary [8, 9], and the uses of solar cells are shown in Figure 1.

Due to the overlap in the metallization structure between the two paste components (AgAl and Al), fire procedures can have a substantial impact on cell strength. Fracture testing revealed that cracks formed in the AgAl/Al overlap zone, causing local stress concentrations that eventually led to fracture at reduced stress levels. Strength tests on typical

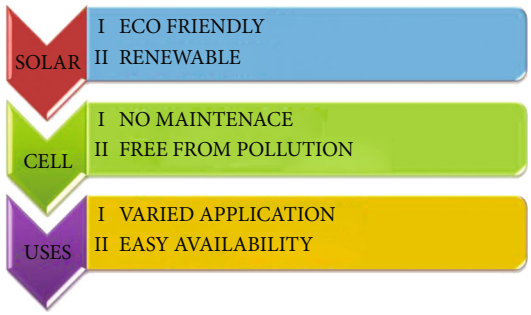

Figure 1: Uses of solar cell.

solar cells were carried out by [10] using 4-point bending and an analytical stress evaluation. Higher drying and lower firing temperatures could be proven to reduce the back-side tensile strength of the solar cell. Aluminium back contact has also been tested for its mechanical qualities [11]. In order to anticipate the maximum deflection of solar cells after discharge, [12] devised this model. Mori–Tanaka homogenization [13] was used to estimate the Al layer's mechanical reaction. Although mechanical models of a solar cell are still lacking, stress 4-point bending tests can be done to examine them [14].

Solar cell strength is determined using a mechanical model that mimics the current standard idea using the H-pattern, Al-BSF [15, 16]. Mechanical homogenization methods are used to examine several aspects of the solar cell layer system, including Al, Si, and Al thin film deposition on the back side [17]. In order to analyze and characterize the bending behaviour and stress fields in solar cells, finite element analysis [18] is utilized, taking into account the different material layers. Al-BSF and the H-pattern solar cells are tested [19] in 4-point bending with varying loads using the FE model and the Weibull analysis [20]. A simulation model constructed using this information was used to study the effective stress on the silicon component of a photovoltaic cell.

2. Material and Methods

2.1. Samples. Solar cells with a diameter of 160 mm, 160 mm, and 220 mm (TTV: 30 mm) were employed for the strength evaluations. Al-BSF, H-pattern, and three busbars were used for the standard concept cells. Material consistency is ensured because all cells come from the same batch. Continuous Ag-busbars with a width of 4 mm and a length of 130 mm created the back-side contact. On the sunny side of the busbars, an alkali perforated coating with an antireflection layer was also found (width 2 mm, length 160 mm) (front side). Table 1 contains more details on the simulation model's material properties.

2.2. Strength Testing. Silicon solar cells can be tested using the same methods as silicon wafers. However, in the literature, it is most commonly used to quantify the strength of wafers. Uniaxial bending moments evenly distribute the stress across a vast surface area, including the sample's edges and surface. A consistent flexural stress is applied to the sample's lower portion. With an outer span of 120 mm, the four-point bend configurations in this study used inner rollers that had a diameter of 60 mm. Steel rollers with a diameter of 12 mm are used in the machine. Among the rollers and the cells, PTFE foils are utilized to improve contact behaviour and reduce friction [21]. When comparing the busbars to the rollers, at the busbars, the rolls feature little slots. During examination, the cell and roller are not separated by foils in the grooves. Table 2 shows the four distinct testing configurations that were carried out.

Ductile tension is applied to the rear and front sides of the solar panels, with the busbars parallel and perpendicular to the rollers. Each design was tested with 60 solar cells. The universal testing equipment was used to conduct all of the tests with a 1 kN load cell. The machine's position was used to determine the sample's deflection. It was decided that the load speed would be 0.1 mm/s. During testing, each sample's power and bending were recorded. A force of 0.5 N was applied to the photovoltaic array before it was broken. To prevent the cells from breaking during 4-point bending testing, strips of sticky tape were applied diagonally to the rollers. A mechanical prototype is utilized to compute the rupture stress during the four-point bending test. To put it another way, the Weibull modulus is a measure of how much the fracture stress values vary over time. This method was used to determine the Weibull parameters using maximum likelihood estimation (MLE).

3. Modeling

3.1. Layer Properties. Different layers are depicted in Figure 2 as part of the solar cell's structure. For the solar cell concept studied here, contact metallizations include screen-printed silver pastes (busbars and fingers) and aluminium pastes (back contact). While burning, aluminium diffused into silicon, creating the eutectic and the back surface field (BSF). AlSi particles that are weakly linked are found in the bulk porous Al layer after fire. Alumina covers these particles. The crystal structure of the silicon in the cell is cubic, whereas the BSF has an Al-doped zone. Doped regions are expected to have identical mechanical properties. Still, the Ag solution used for transmission lines and fingers has a more homogeneous microstructure than the Al layer on the backside. Researchers employed the Mori–Tanaka approach to conduct theoretical mechanical studies on eutectic and Al pastes to homogenize the elastic modulus. According to the theoretical calculations, AlSi has a Young's modulus of 74 GPa in its eutectic layer.

Modeling silicon relies on continuous elastic properties, whereas other levels are represented as brittle materials that can be deformed. Ag paste's optimal rigidity and production stresses were found to be at 41.5 MPa for Al paste. We can see how the Al paste fractures on the interface among the elements and the glass by using a spherical particle as an example. Furthermore, the weak interparticle forces are thought to be a result of the porous structure. Thus, it is hypothesized that the solar cell's stress behaviour in compression is predominantly influenced by the porous Al,

Table 1: The mechanical model's material parameters.

Layer	Material	Young's modulus E (GPa)	Poisson's ratio ν	Thickness of layer $t(\mu m)$
Front-side busbars	Silver	8	0.41	12
Silicon	Silicon	$C_{11} = 172.6$, $C_{12} = 64.86$, $C_{44} = 81.24$	0.29	≈215
Eutectic layer	Aluminium silicon	76	0.42	4
Back-side Al paste	Por. Al	7	0.40	30
Busbars on back side	Silver	8	0.41	30

Table 2: Solar cell strength testing in four-point bending is performed using batches and configurations of samples.

Name	Side in tensile stress	Position rollers to busbars	Cell numbers	Direction of tensile stress to busbars
SP	Sunny side	Lateral	60	Transverse
SC	Sunny side	Transverse	60	Lateral
BP	Back side	Lateral	60	Transverse
BC	Back side	Transverse	60	Lateral

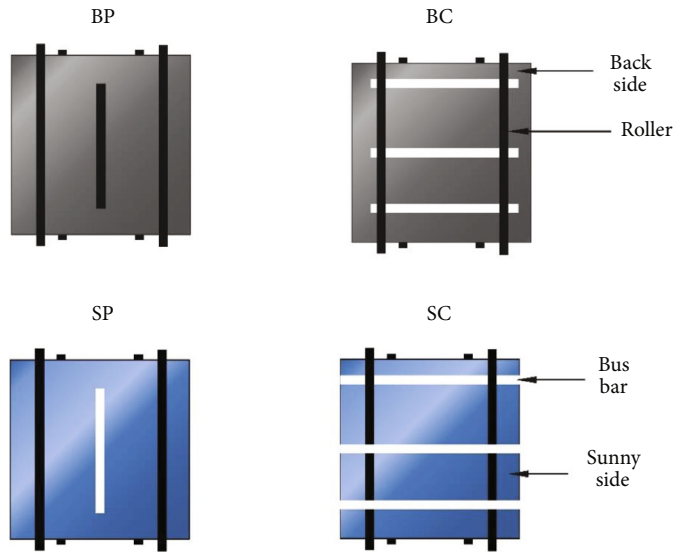

Figure 2: Detailed diagrams of all of the configurations used for strength testing.

while the cell's stress behaviour in tension is more susceptible to failure. As the system compresses, the AlSi particles may contribute a little amount of stiffness. To determine cell breakage, it has been assumed that the silicon layer breaks. As a failure criterion, the highest possible primary stress is employed. Further, it is thought that flaws on the silicon layer's surface cause fracture at the silicon layer. As a result, the solar cell's fracture is not due to another layer in the solar cell.

3.2. Mechanical Model. Displacements and the photovoltaic panels under frustration were calculated using the FE casing structure that was constructed in the ANSYS finite element (FE) programme and shown in Figure 3. Silicon's mechanical properties are not affected by the BSF; hence, it is not shown as a solitary framework. Because the anti-reflective coating on the top side is so thin, it is not taken into account. Small grids of Ag on the solar cell's upper surface are also ignored because of their inconsequential impact on the cell's stiffness and stress distribution. This simulation model does not take into account residual stresses after thermal processing, the values of which are taken to remain constant throughout all samples. The calculated stress fields can then be superimposed with these new stresses. There are nodes, and the photovoltaic cell's levels are partitioned in the FE model's shell elements. Silicon, on the other hand, is regarded as a linear elastic isotropic material. As shown in Table 1, the elastic constants of silicon are represented using Voigt's notation for anisotropic linear elastic behaviour (f100g crystal orientation). Ductile layers' plastic material behaviour was ignored since stress levels in the ductile layers did not exceed yield stresses. The simulation prototype additionally accounts for nonlinearities as well as massive deflection contact and friction among the rollers of the four-point bending test system. To get the best results, choose a coefficient of friction equal to 0.18.

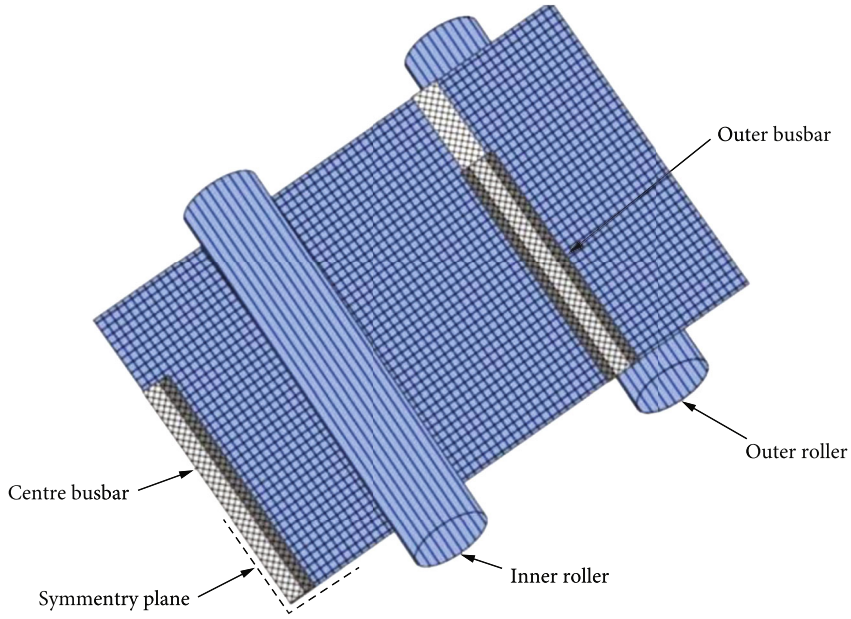

Figure 3: FEM model in quarter symmetry with mesh shell elements and different sections for different layers with busbars parallel to the roller.

4. Results

4.1. Resulting Numbers from Simulation. Deflection, which characterizes the solar cell's structural behaviour, serves as the model's load parameter. If you compare the same pattern of pure silicon substrate on a silicon wafer as a silicon layer within a cell, a 10 mm deflection exhibits the maximum stress (first major stress on the ductile side of the silicon layer) and as an example of where a silicon wafer's loading force compares to a pure silicon substrate. The stiffness (force) of silicon among a wafer and a cell is reduced by <3%. There is just a small amount of stress in the surrounding metallization layers that affects the maximum stress in the silicon. When it comes to stress concentrations at metallization–silicon interfaces, however, the shell model cannot account for them. Despite this, simulations can be used to predict whether a photovoltaic works using the same assumptions as for pure silicon wafers. In this case, the fracture stresses were calculated using the mechanical solar cell model, which took into account the number of cosystem's consequences. The roller force vs. deformation curves from study were analyzed to those from the simulated world in order to verify the quantitative instances of 4-point bending tests. The experiment's nonlinear curve progression can be characterized via simulation, as can be seen. Experimental results and computer simulations show that the pastes in Table 2 have a satisfactory overall stiffness. 0.5 N was the starting point for the experiment's experimental curve because of the initial force used.

4.2. The Results of Testing for Strength. Deformation constraints were calculated using a simulation framework on the fracture's power and diversion. Weibull criteria for the four topologies illustrated in Table 3 were determined using these stressors. Fault stresses are sprinkled by the Weibull

Table 3: Weibull parameters of strength with 90% confidence bounds were obtained by four-point bending experiments using solar cells in various configurations.

Tensile stress side	Busbar roller positions	m	σ_θ (MPa)
Sunny side	Transverse	15	201
Sunny side	Lateral	16	204
Back side	Transverse	15	246
Back side	Lateral	18	172

modulus, which was not significantly different in any of the varied designs. Defects are evenly distributed among all samples as a result of this. Neither significant difference between layouts across or parallel to busbars when tensile stress is applied to the sunny side. To put it another way, rollers perpendicular to busbars have a higher typical fracture stress than rollers parallel to the busbars. Since the metallization layers are taken into consideration, these fracture stress values can be used to evaluate the absolute strength of the use of photovoltaics (neglecting residual stress states). Examination of shattered cells led to the use of optical tools to inspect the cells. The back-side metallization connects each cell even if the sunny side is checked. EL is more difficult to conduct on the underside of the solar cell, which shatters more quickly. In the preferred cleavage planes (112) or (113) of silicon, all cracks propagate in a 460 degree angle. Many minor cracks were found in a region of continual flexure (among the red lines) during testing on the sunny side. If you look closely, you will find two distinct lines of cracks running in opposite directions on the surface of the busbars, which is where the cracks originate. For SP design, a single break can spread across the cell's thickness. The origin is more difficult to find if the back side is examined, as large regions are not electrically connected. Back-side testing shows that cracks

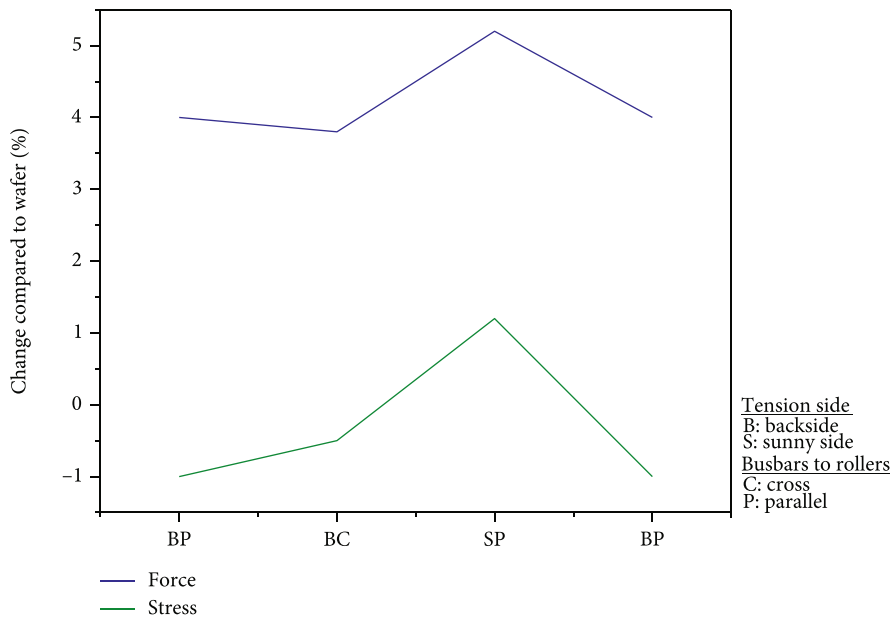

Figure 4: Rollers of variant solar cell designs at 10 mm bending have the highest first primary stress and response force of pure silicon (wafer) of the same thickness.

commonly spread in two directions from busbars for the optical inspection, indicating that the transmission lines and the pore structure are where the cracks begin. As observed in the EL photos, back-side testing results in a lesser number of cracks than sunny-side testing.

5. Elaboration

5.1. Loading Direction Affects the Strength of a Load. Figure 4 shows that the rollers of variant solar cell designs at 10 mm bending have the highest first primary stress and response force of pure silicon (wafer) of the same thickness. For perforated polycrystalline silicon because of defects in the silicon, they are unusable in the resin coating form, since the durability of the sunshine end of solar cells is irrespective of the beam axis. On the other hand, the loading direction has a significant impact on the strength of the back side. The creation of a eutectic layer, however, does not change the busbar's direction dependency, despite the fact that the flaws on the surface have been altered. Figure 5 shows the rollers' force vs. displacement curves. The comparison of the (a) SP configuration specimen in simulation and experiment and (b) all configurations in the experiment.

Figure 6 shows that the local stress concentrations in 3D models cannot explain the disparity in BC and BP strength. Busbars and Al paste appear to be controlled by their metallization mechanism. Finding similar statistics on the maximum load orientation contributes to the effectiveness of solar cells being not possible. Four-point bending tests on typical solar cells just for the back and front sides were conducted as in Table 3. They [6] evaluated a variety of ring–on–ring test configurations of metallizations. It is not possible to directly compare axisymmetric stress to biaxial stress in this test because of the nature of the 4-point bending test. They [22] discovered that the strength of an aluminium busbar differs depending on whether it is perpendicular or parallel to the aluminium back paste [23]. Cracks can be found in the overlap area between the Al and Ag pastes in the BC configuration. It was tested on a smaller sample of solar cells and busbars in the BC arrangement. These samples were shattered into two pieces during shipping. The back-side paste and busbars were discovered to be the source of the cracks in these samples. Cracks caused by stress concentrations in the delamination of material layers were also found to be similar. These cracks are more likely to form at high-stress circumstances, as is the case with the BC framework in 4-point bending. These overlap cracks, however, may be affected by the composition of the busbar and rear contact adhesive.

So far, the mechanical model has ignored the effects of manufacturing residual stresses. Tensile stresses from the front side of silicon and flexural rigidity stresses on the rear are expected as a result of heat treatment shear strength. The rear side might have a substantially minor crack stress, whereas the front end could take a greater relative crack stress. Peripheral shear forces, such as those caused by overlying anodization layers, might have an effect on the direction of the residual stress components in a component design. Consider these points in greater detail. Cell breakage is more pronounced when the same loads are applied parallel to the busbars. Although soldering and lamination in modules may have an impact on failure mechanisms, this is not a certainty. Because modules put the entire cell under tensile stress, it is impossible to compare them.

5.2. Fracture Behaviour Influenced by Layering. Associated to the back end in tensile stress, the sunny side of the cell reveals a lot more cracks that do not separate the complete thickness of the cell, which includes the metal. Cracks were also seen on the back side of the board when it was arranged in parallel rather than perpendicular orientation. For example,

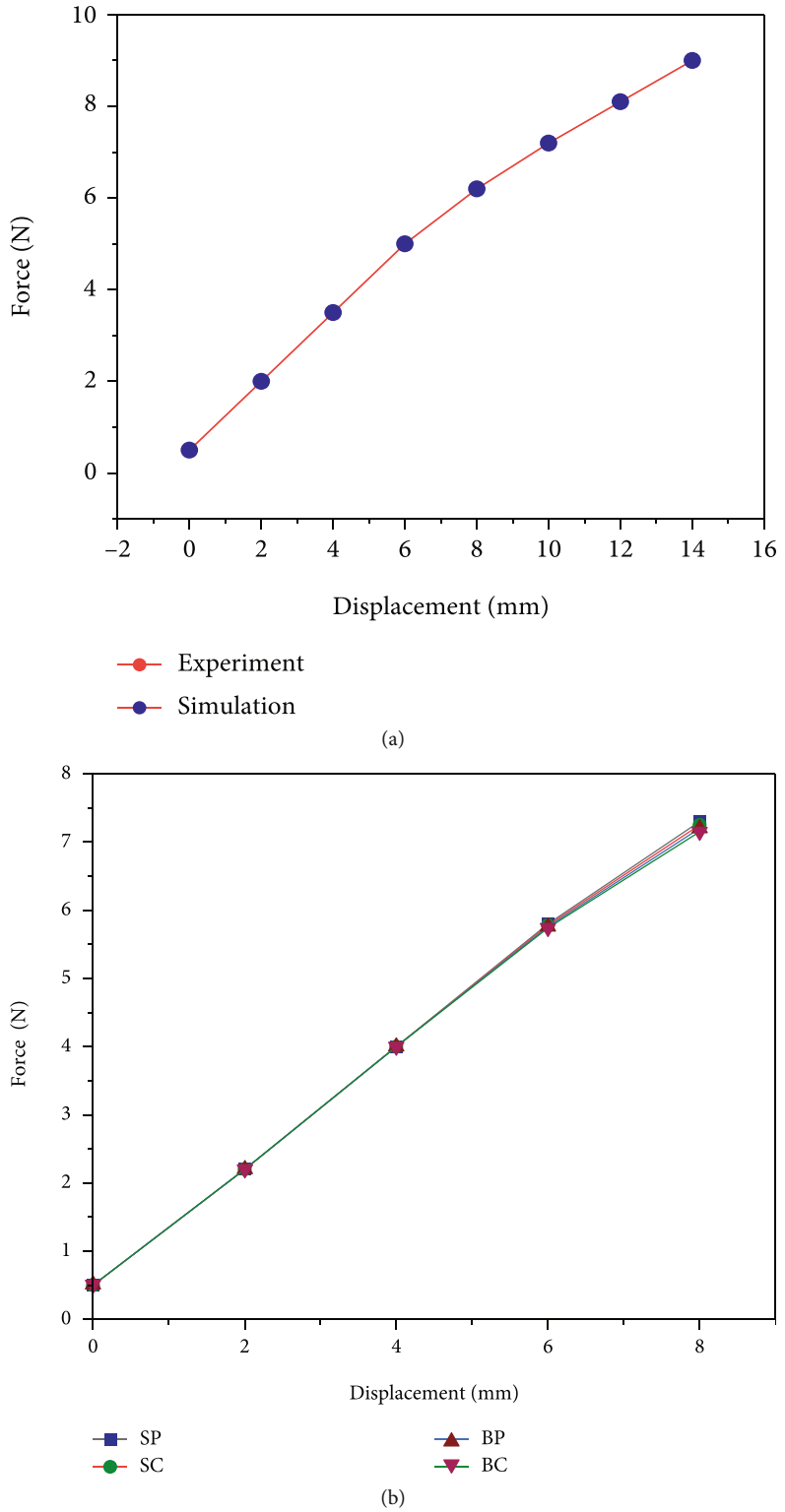

Figure 5: The rollers' force vs. displacement curves. The comparison of the (a) SP configuration specimen in simulation and experiment and (b) all configurations in the experiment.

the elastic energy in a solar cell could explain how a crack branching or many crack origins can occur. As a result, energy can be employed to propagate multiple cracks in materials tested on the sunny side. Back-side tests break the cell, causing elastic energy to be lost because the silicon pieces are no longer connected. As a result of the higher energy available, additional branched cracks will form on the back side in parallel formation. Cracks appeared close and corresponding to the busbar in all 4-point bending configurations other than the SP configuration. If the fracture travels in cleavage planes of

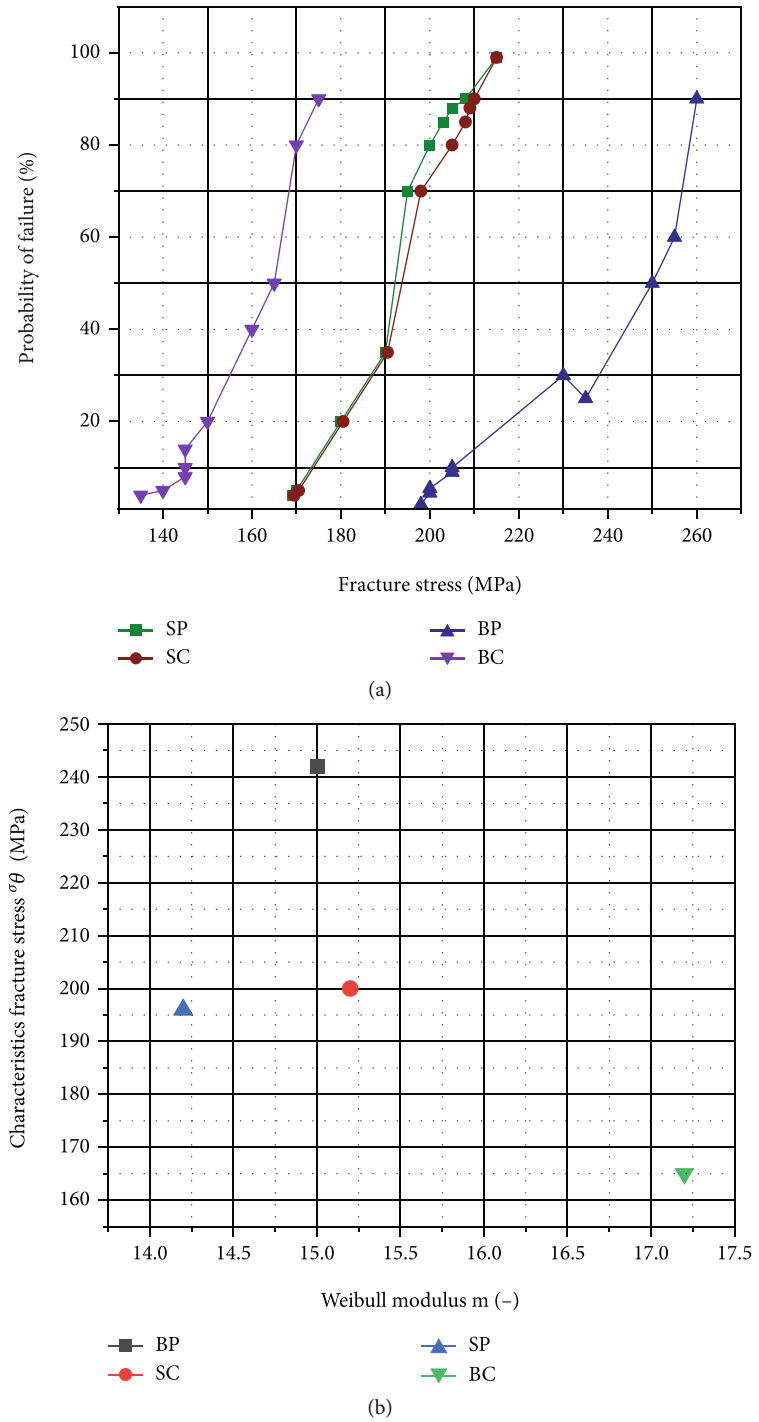

Figure 6: Analysis of four-point bending tests using solar cell in various parameters. MLE (a) Weibull drawing and (b) Weibull constraints with 95% assurance intervals are provided.

silicon, a fault or remaining stress near the busbar is likely to be the cause of this particular crack propagation. Despite the huge crack near the busbar, the two front-side layouts are indistinguishable in terms of their structural integrity. The occurrence of two fractures on the back-side arrangement indicates that a crack originated near the busbars. These cracks do not propagate similar to busbars, unlike the SP design.

6. Conclusions

The layered structure can be considered in this study; however, it has only a little influence on the stiffness and stress distribution of the solar cell. The model, on the other hand, may be used to correctly and precisely estimate the fracture stress of solar cells. This model may also be used to

investigate different metallization processes on various solar cell designs:

(i) Square crystalline silicon solar cells were exposed to four-point bending examinations with rear and sunny sides under tensile stress in order to determine their tensile strength

(ii) The Weibull modulus of all configurations was the same, which can be taken as a similar defect distribution for all of them. If the rollers are parallel or perpendicular to busbars, the characteristic fracture stress is not much different

(iii) Tensile stress on back side of perpendicular rollers is stronger than that on parallel ones. To put it another way, the metallization structure of solar cells appears to have a direct impact on the cell's strength

(iv) The loading direction in the current standard solar cells is unaffected by the direction of the sun. Because of this, the strength of the back side varies depending on which way it is being loaded

(v) In future efforts, the Al and Ag pastes overlapping can be investigated further. Breakage of photovoltaic modules can be studied by bending the modules to examine the cracking of solar cells in modules

Data Availability

The data used to support the findings of this study are included within the article. Further data or information is available from the corresponding author upon request.

Conflicts of Interest

The authors declare that there is no conflict of interest regarding the publication of this article.

Acknowledgments

The authors appreciate the support from Ambo University, Ethiopia, for providing help during the research and preparation of the manuscript. The authors thank Sri Sairam Engineering College, RMK College of Engineering and Technology, for providing assistance to this work. The authors would like to acknowledge the Researchers Supporting Project number (RSP-2021/373), King Saud University, Riyadh, Saudi Arabia.

References

[1] A. Veera Kumar, T. V. Arjunan, D. Seenivasan, R. Venkatramanan, and S. Vijayan, "Thermal performance of an evacuated tube solar collector with inserted baffles for air heating applications," *Solar Energy*, vol. 215, pp. 131–143, 2021.

[2] M. Köntges, I. Kunze, S. Kajari-Schröder, X. Breitenmoser, and B. Bjørneklett, "The risk of power loss in crystalline silicon based photovoltaic modules due to micro-cracks," *Solar Energy Materials & Solar Cells*, vol. 95, no. 4, pp. 1131–1137, 2011.

[3] K. Wasmer, A. Bidiville, F. Jeanneret et al., "Effects of Edge Defects Induced by Multi-Wire Sawing on the Wafer Strength," in *23rd European Photovoltaic Solar Energy Conference*, pp. 1305–1310, Valencia, 2008.

[4] A. Bohne, S. Schoenfelder, C. Hagendorf, D. Schmidt, and J. Bagdahn, "The influence of the wire sawing process on mono-and multicrystalline silicon wafers," in *Proceedings of 23rd PVSEC*, pp. 1780–1784, Spain, 2008.

[5] B. Klusemann, H. J. Böhm, and B. Svendsen, "Homogenization methods for multi-phase elastic composites with non-elliptical reinforcements: comparisons and benchmarks," *European Journal of Mechanics-A/Solids*, vol. 34, pp. 21–37, 2012.

[6] C. Kohn, T. Faber, R. Kübler et al., "Analyses of Warpage Effects Induced by Passivation and Electrode Coatings in Silicon Solar Cells," in *22nd European Photovoltaic Solar Energy Conference and Exhibition*, pp. 1–10, Milan, Italy, 2007.

[7] T. Behm, W. Fütterer, C. Funke et al., "Challenges of the wire saw wafering process," *Photovoltaics International*, vol. 11, pp. 36–47, 2011.

[8] A. Grün, A. Lawerenz, R. Porytskyy, and O. Anspach, "Investigation of wafer surfaces with space-resolved breaking strength tests and corresponding analysis of the crack depth," in *26th EU PVSEC*, pp. 2116–2119, Hamburg, 2011.

[9] H. Wu, S. N. Melkote, and S. Danyluk, "Mechanical strength of silicon wafers cut by loose abrasive slurry and fixed abrasive diamond wire sawing," *Advanced Engineering Materials*, vol. 14, no. 5, pp. 342–348, 2012.

[10] F. Kaule, W. Wang, and S. Schoenfelder, "Modeling and testing the mechanical strength of solar cells," *Solar Energy Materials & Solar Cells*, vol. 120, pp. 441–447, 2014.

[11] C. Kohn, R. Kübler, M. Krappitz et al., "Influence of the metallization process on the strength of silicon solar cells," in *24th European Photovoltaic Solar Energy Conference*, p. 25, Hamburg, Germany, 2009.

[12] V. A. Popovich, M. Janssen, J. Bennett, and I. M. Richardson, "Breakage issues in silicon solar wafers and cells," *Photovoltaics International*, vol. 12, pp. 49–57, 2011.

[13] V. A. Popovich, M. Janssen, I. M. Richardson, T. Van Amstel, and I. J. Bennett, "Microstructure and mechanical properties of aluminum back contact layers," *Solar Energy Materials & Solar Cells*, vol. 95, no. 1, pp. 93–96, 2011.

[14] T. Van Amstel, V. A. Popovich, P. C. de Jong, and I. J. Bennett, "A Multiscale Model of the Aluminium Layer at the Rear Side of a Solar Cell," in *Proceedings of the 23rd European Photovoltaic Solar Energy Conference*, pp. 1–12, Hamburg, Germany, 2009.

[15] A. Veera Kumar, T. Arjunan, D. Seenivasan, R. Venkatramanan, and S. Vijayan, "Techno-economic evaluation of an evacuated tube solar air collector with inserted baffles," *Proceedings of the Institution of Mechanical Engineers, Part E: Journal of Process Mechanical Engineering.*, vol. 235, no. 4, pp. 1027–1038, 2021.

[16] W. Weibull, "A statistical distribution function of wide applicability," *Journal of Applied Mechanics*, vol. 18, no. 3, pp. 293–297, 1951.

[17] S. Schoenfelder, A. Bohne, and J. Bagdahn, "Comparison of test methods for strength characterization of thin solar wafer," *Proceedings of the 22nd European Photovoltaic Solar Energy Conference*, vol. 1, pp. 1636–1640, 2007.

[18] E. Din, *843-2 Hochleistungskeramik–Mechanische Eigenschaften monolithischer Keramik bei Raumtemperatur–Teil 2:*

Bestimmung des Elastizitätsmoduls, Schubmoduls und der Poissonzahl, 2007.

[19] J. Krause, R. Woehl, M. Rauer, C. Schmiga, J. Wilde, and D. Biro, "Microstructural and electrical properties of different-sized aluminum-alloyed contacts and their layer system on silicon surfaces," *Solar Energy Materials & Solar Cells*, vol. 95, no. 8, pp. 2151–2160, 2011.

[20] V. A. Popovich, N. Van Der Pers, M. Janssen et al., "Residual and bending stress measurements by X-ray diffraction and synchrotron diffraction analysis in silicon solar cells," in *2012 38th IEEE Photovoltaic Specialists Conference*, pp. 442–447, Austin, TX, USA, 2012.

[21] M. Pander, *Mechanische Untersuchungen an Solarzellen in PV-Modulen mittels Finite-Elemente-Modellierung*, Hochschule für Tech, Wirtschaft und Kul, Leipzig, Germany, 2010.

[22] J. J. Hall, "Electronic effects in the elastic constants of n-type silicon," *Physics Review*, vol. 161, no. 3, pp. 756–761, 1967.

[23] M. Sander, S. Dietrich, M. Pander, M. Ebert, and J. Bagdahn, "Systematic investigation of cracks in encapsulated solar cells after mechanical loading," *Solar Energy Materials & Solar Cells*, vol. 111, pp. 82–89, 2013.